

UCSF

UC San Francisco Previously Published Works

Title

Stem cell marker (Nanog) and Stat-3 signaling promote MicroRNA-21 expression and chemoresistance in hyaluronan/CD44-activated head and neck squamous cell carcinoma cells.

Permalink

<https://escholarship.org/uc/item/2527j0wd>

Journal

Oncogene, 31(2)

ISSN

0950-9232

Authors

Bourguignon, LYW
Earle, C
Wong, G
et al.

Publication Date

2012

DOI

10.1038/onc.2011.222

Peer reviewed



Published in final edited form as:

Oncogene. 2012 January 12; 31(2): 149–160. doi:10.1038/onc.2011.222.

Stem Cell Marker (Nanog) and Stat-3 Signaling Promote MicroRNA-21 Expression and Chemoresistance in Hyaluronan/CD44-activated Head and Neck Squamous Cell Carcinoma Cells

Lilly Y. W. Bourguignon[#], Christine Earle, Gabriel Wong, Christina C. Spevak, and Katherine Krueger

San Francisco Veterans Affairs Medical Center and Department of Medicine, University of California at San Francisco & Endocrine Unit (111N2), 4150 Clement Street, San Francisco, CA 94121

Abstract

MicroRNAs are often associated with the pathogenesis of many cancers including Head and Neck Squamous Cell Carcinoma (HNSCC). In particular, microRNA-21 (miR-21) appears to play a critical role in tumor cell survival, chemoresistance and HNSCC progression. In this study we investigated matrix hyaluronan (HA)-induced CD44 (a primary HA receptor) interaction with the stem cell markers, Nanog and Stat-3, in HNSCC cells (HSC-3 cells). Our results indicate that HA binding to CD44 promotes Nanog-Stat-3 (also tyrosine phosphorylated Stat-3) complex formation, nuclear translocation and transcriptional activation. Further analyses reveal that miR-21 is controlled by an upstream promoter containing Stat-3 binding site(s), while chromatin immunoprecipitation (ChIP) assays demonstrate that stimulation of miR-21 expression by HA/CD44 signaling is Nanog/Stat-3-dependent in HNSCC cells. This process results in a decrease of a tumor suppressor protein (PDCD4), and an upregulation of inhibitors of the apoptosis family of proteins (IAPs) as well as chemoresistance in HSC-3 cells. Treatment of HSC-3 cells with Nanog-and/or Stat-3-specific small interfering RNAs (siRNAs) effectively blocks HA-mediated Nanog-Stat-3 signaling events, abrogates miR-21 production and increases PDCD4 expression. Subsequently, this Nanog-Stat-3 signaling inhibition causes downregulation of survival protein (IAP) expression and enhancement of chemosensitivity. To further evaluate the role of miR-21 in tumor cell-specific functions, HSC-3 cells were also transfected with a specific anti-miR-21 inhibitor in order to silence miR-21 expression and block its target functions. Our results demonstrate that anti-miR-21 inhibitor not only upregulates PDCD4 expression, but also decreases IAP expression and enhances chemosensitivity in HA-treated HNSCC cells. Together, these findings indicate that the HA-induced CD44 interaction with Nanog and Stat-3 plays a pivotal role in miR-21 production leading to PDCD4 reduction, IAP upregulation and chemoresistance in HNSCC cells. This novel Nanog/Stat-3 signaling pathway-specific mechanism involved in

Users may view, print, copy, download and text and data- mine the content in such documents, for the purposes of academic research, subject always to the full Conditions of use: http://www.nature.com/authors/editorial_policies/license.html#terms

[#]Reprint requests should be addressed to: Dr. Lilly Y.W. Bourguignon, Endocrine Unit (111N), Department of Medicine, University of California at San Francisco and VA Medical Center, 4150 Clement Street, San Francisco, CA 94121, TEL: (415) 221-4810 x 3321, FAX: (415) 383-1638, lilly.bourguignon@ucsf.edu.

CONFLICT OF INTEREST: All authors declare no conflict of interest.

miR-21 production is significant for the formation of future intervention strategies in the treatment of HA/CD44-activated HNSCC.

Keywords

Nanog; Stat-3; miR-21; hyaluronan; CD44; head & neck cancer

INTRODUCTION

Head and neck squamous cell carcinoma (HNSCC) is a malignancy that involves cancers of the lip, oral cavity, pharynx, hypopharynx, larynx, nose, nasal, sinuses, neck, ears and salivary glands (Parkin, et al., 2005). Advanced HNSCC is an aggressive disease associated with major morbidity and mortality. The three-year survival rate for patients with advanced-stage HNSCC treated with standard therapy is only 30 to 50%. Resistance to standard therapy continues to be a limiting factor in the treatment of HNSCC. Nearly 40 to 60% of HNSCC patients subsequently develop chemoresistance, locoregional recurrences or distant metastases (Jemal, et al. 2008; Parkin, et al. 2005). Thus, clarification of key aspects of tumor cell functions underlying the clinical behavior of HNSCC is greatly needed.

Previous studies identified specific extracellular matrix (ECM) components in head and neck squamous cell carcinoma (HNSCC) that correlate with tumor cell behaviors (Wang and Bourguignon, 2011). Among such candidate molecules is hyaluronan (HA) which is a nonsulfated, unbranched glycosaminoglycan consisting of repeating disaccharide units, D-glucuronic acid and N-acetyl-D-glucosamine (Toole and Hascall, 2002). HA interacts with CD44, a family of cell-surface glycoprotein receptors which are also expressed in a variety of human solid neoplasms, particularly those classified as HNSCC (Wang, et al., 2009). Both CD44 and HA are overexpressed/elevated at sites of tumor attachment (Toole and Hascall, 2002; Toole, et al., 2002). HA binding to CD44 not only affects cell adhesion to extracellular matrix (ECM) components, but also is involved in the stimulation of a variety of tumor cell-specific functions leading to cytoskeleton function and HNSCC progression (Turley, et al., 2002; Bourguignon, 2008). However, the oncogenic mechanism(s) occurring during HA-activated and CD44-specific HNSCC progression remain(s) to be determined.

The stem cell marker, Nanog is an important transcription factor involved in the self-renewal and maintenance of pluripotency in the inner cell mass (ICM) of mammalian embryo and of embryonic stem (ES) cells (Mitsui, et al., 2003). Nanog signaling is regulated by interactions among various pluripotent stem cell regulators (e.g., Rex1, Sox2 and Oct3/4) which together control the expression of a set of target genes required for ES cell pluripotency (Mitsui, et al., 2003). These findings confirm the essential role of Nanog in regulating a variety of cellular functions. Recently, several tumor cell types have been shown to express Nanog (Ezeh, et al., 2005; Bourguignon, et al., 2008). HA binding to epithelial tumor cells has been shown to promote Nanog protein association with CD44, followed by Nanog activation and the expression of pluripotent stem cell regulators (e.g., Rex1 and Sox2) (Bourguignon, et al., 2008). These findings strongly suggest that HA/CD44 signaling and Nanog function are tightly linked.

The “signal transducer and activator of transcription protein 3” (Stat-3) was initially identified as APRF (Acute Phase Response Factor), an inducible DNA binding protein that binds to the IL-6-responsive element within the promoters of hepatic acute phase genes (Darnell, 1997, Heinrich, et al., 2003). Accumulating evidence indicates that Stat-3 also plays an important role in regulating cell growth, differentiation, and survival (Huang, 2007). Nanog and Stat-3 also appear to be both structurally linked and functionally coupled in HA/CD44 signaling during epithelial tumor cell activation (Bourguignon, et al., 2008). The question of whether Nanog and Stat-3 are interacting with each other in HNSCC cells will be addressed in this study.

A number of studies indicate that more than 50% of microRNA [(miRNA), small RNA molecules with ~20–25 nucleotides] are located in cancer-related genomic regions or fragile sites, suggesting that miRNA may be closely associated with the pathogenesis of a variety of cancers including HNSCC (Chang, et al., 2008; Volinia, et al., 2006). Analysis of an array profile of miRNA expression in HNSCC tissues reveals that miR-21 is abundantly produced in these tumors compared to normal tissues (Volinia, et al., 2006). The functional significance of miR-21 has been elucidated in several recent studies following the discovery of its specific targets (Asangani, et al., 2008), making miR-21 one of the most-studied miRNAs due to its involvement in cancer progression. Importantly, miR-21 plays a role in the inhibition of tumor suppressor proteins such as Program Cell Death 4 (PDCD4), via a conserved site within the 3'-UTR (3'-untranslated region) of the mRNA (Asangani, et al., 2008; Bourguignon, et al., 2009a). Downregulation of PDCD4 expression by miR-21 leads to tumor cell growth, survival, chemoresistance, invasion and metastasis (Bourguignon, et al., 2009a). Thus, miR-21 is currently considered to be an oncogenic miRNA. Whether HA/CD44-mediated Nanog (or Stat-3) signaling is involved in regulating oncogenic miRNA (e.g., miR-21) expression/function and tumor-specific behaviors in HNSCC cells has not been determined, and represents the primary focus of this study.

In this study we discovered a new matrix HA/CD44-mediated Nanog/Stat-3 signaling mechanism that regulates miR-21 production and chemoresistance in HNSCC cells. Specifically, our results indicate that HA/CD44 activates Nanog-Stat-3 signaling which, in turn, stimulates miR-21 expression and function. These events lead to the reduction of the tumor suppressor protein, PDCD4, upregulation of survival proteins and cisplatin chemoresistance in HNSCC cells. Inhibition of either Nanog/Stat-3 signaling or silencing miR-21 expression/function not only results in PDCD4 upregulation, but also causes a reduction of survival protein expression and an enhancement of chemosensitivity to cisplatin. Thus, our findings strongly support the contention that Nanog, Stat-3, and miR-21 form a functional signaling axis that regulates tumor cell survival and cisplatin chemoresistance in HNSCC cells.

RESULTS

HA-mediated CD44 interaction with Nanog and Stat-3 in HSC-3 Cells

Previous studies showed that both Nanog and Stat-3 are functionally coupled during oncogenesis (Bourguignon, et al., 2008). Among the signaling aberrations present in HNSCC, Stat-3 activation appears to be one of the critical pathways in HNSCC

development and progression (Song and Grandis, 2000). Cellular transformation by Stat-3 generally requires specific phosphorylation of the tyrosine 705(pY705) residue (Wen, et al., 1995). In this study we first examined whether Nanog and Stat-3 are expressed in clinical HNSCC tissue specimens. Primary HNSCC tumors were immunostained with antibodies for Nanog, total Stat-3 and tyrosine phosphorylated Stat-3. Fig. 1A shows representative examples of the immunohistochemical staining of HNSCC primary tumors for both Nanog and Stat-3 (Fig. 1A-a & b). We have also observed co-localization of Nanog with tyrosine phosphorylated Stat-3 and total Stat-3 (Fig. 1A-c-e and Fig. 1A-f-h) in HNSCC patient samples. These findings clearly demonstrated that a close association between Nanog and Stat-3 (including tyrosine phosphorylated Stat-3) occurs in head and neck cancer patient samples.

HA/CD44-mediated oncogenic signaling has been implicated in both the initiation and development of several solid tumors including head and neck cancer (Bourguignon, et al., 2008, 2009a; Huang, 2007; Toole and Hascall, 2002; Wang, et al., 2009; Wang and Bourguignon, 2011). However, the cellular and molecular mechanisms by which HA/CD44 signaling occurs in HNSCC cells are still poorly understood. In this study we have focused on the question of whether there is a physical linkage between CD44 and tyrosine phosphorylated Stat-3[pY705] in HNSCC cells [e.g., HSC-3 cell line (Fig. 1)]. To this end we performed a HA-mediated Stat-3 tyrosine phosphorylation time course (e.g., 0, 5, 15 and 60min) using anti-CD44-mediated immunoprecipitation followed by anti-Stat-3[pY705] immunoblot or anti-CD44 immunoblot, respectively. Our results indicate that the association of phosphorylated Stat-3 with CD44 occurs as early as 5min following HA addition to HNSCC cells (Fig. 1B).

Next, we investigated whether there is an interaction between Nanog and total Stat-3 in the CD44-associated signaling complex in HNSCC cells [e.g., HSC-3 cells (Fig. 1C)]. Specifically, we performed anti-CD44-mediated immunoprecipitation followed by anti-Nanog immunoblot or anti-total Stat-3/anti-Stat-3[pY705] immunoblot or anti-CD44 immunoblot (Fig. 1C), respectively, using cells treated with HA or without HA. Our results indicate that a 5min HA treatment causes the recruitment of Nanog and total Stat-3 (together with tyrosine phosphorylated Stat-3) (Fig. 1C-a,b, c) into the CD44 complex (Fig. 1C-d). In contrast, a low level of Nanog or Stat-3 (or tyrosine phosphorylated Stat-3) is present in the anti-CD44-immunoprecipitated materials (reblotted with anti-CD44) in cells not treated with HA (Fig. 1C-a, b, c, d) or in cells pretreated with anti-CD44 antibody followed by a 5min HA treatment (Fig. 1C-a, b, c, d). These findings clearly establish that CD44, Nanog and Stat-3 (in particular, tyrosine phosphorylated Stat-3) are closely associated with each other, and that there is a significant increase in the recruitment of Nanog, Stat-3 (also phosphorylated Stat-3) into the CD44-associated complex following a 5min HA treatment of HSC-3 cells.

Elucidate Nanog/Stat-3 nuclear translocation, complex formation and transcription activation in HNSCC cells following HA-CD44 binding

Several studies have suggested the importance of HA/CD44-mediated nuclear translocation of transcription factors in regulating target gene expression and tumor cell activation

(Bourguignon, et al. 2008; Bourguignon, et al. 2009a and 2010). In this study using immunofluorescence staining and confocal microscopy, we observed that both Nanog and Stat-3 can be translocated from the cytosol to the nucleus after 15 min HA treatment (Fig. 2A). In contrast, the majority of Nanog and Stat-3 is distributed in the cytosol and only a low level of Nanog and Stat-3 is present in the nucleus of HSC-3 cells, either pretreated with anti-CD44 antibody plus HA (Fig. 2A) or without any HA treatment (Fig. 2A). These observations indicate that HA-CD44 interaction promotes Nanog and Stat-3 nuclear translocation in HNSCC cells.

In order to examine whether Nanog interacts with Stat-3 (in particular tyrosine phosphorylated Stat-3) directly in the nucleus of HSC-3 cells, we analyzed the anti-Nanog-mediated immunoprecipitates from nuclear extracts by immunoblotting with anti-total Stat-3/anti-p-Stat-3[pY705], or anti-Nanog antibody, respectively. Our results demonstrate that very little amount of Nanog is complexed with either total Stat-3 or tyrosine phosphorylated Stat-3 in the nuclear fractions of HSC-3 cells without any HA treatment (Fig. 2B-a, b, c). Importantly, we observed that a 15 min HA treatment of HSC-3 cells stimulates a measurable increase in the amount of Nanog and total Stat-3/tyrosine phosphorylated Stat-3 complexes (Fig. 2B-a, b, c) in the nuclear fractions of HSC-3 cells. When these tumor cells were pretreated with anti-CD44 antibody followed by a 15min HA treatment, the complex formation between Nanog and total Stat-3/tyrosine phosphorylated Stat-3 in the nuclear fraction is greatly reduced in HSC-3 cells (Fig. 2B-a, b, c). These findings suggest that Nanog is capable of forming with Stat-3 (in particular, tyrosine phosphorylated Stat-3) (in the nucleus) in a HA-dependent and CD44-specific manner in HSC-3 cells.

Role of Stat-3 in regulating miR-21 expression in HA/CD44 and Nanog-activated HSC-3 cells

(1) In vivo binding of Stat-3 to the upstream/enhancer region of the miR-21 promoter in HSC-3 cells—A previous study indicated that the gene encoding oncogenic miR-21 is regulated by an upstream/enhancer promoter containing Stat-3 binding sites (Löffler D, 2007). To examine whether Nanog-associated Stat-3 directly interacts with the upstream/enhancer region of miR-21 promoter, anti-Stat-3 antibody-, anti-phospho-Stat-3[pY⁷⁰⁵] and anti-Nanog antibody-specific chromatin immunoprecipitation (ChIP) assays were performed in HSC-3 cells. As shown in Fig. 3, the PCR from both anti-Stat-3, anti-phospho-Stat-3[pY⁷⁰⁵] and anti-Nanog-mediated precipitations from HA-treated HSC-3 cells resulted in a specific amplification product using primer pair specific for the miR-21 promoter/enhancer region containing the Stat-3 binding sites (Fig. 3A-a, b, c, lane 2). In contrast, reduced amount of Nanog is associated with the Stat-3 or phospho-Stat-3 binding of miR-21 upstream/enhancer promoter region in cells pretreated with anti-CD44 antibody followed by HA addition (Fig. 3A-a,b,c, lane 3), or without HA treatment (Fig. 3a,b,c, lane 1). These findings suggest that the recruitment of Stat-3 (also phospho-Stat-3) and Nanog into the upstream/enhancer region of miR-21 promoter site is HA-specific and CD44-dependent.

To confirm the direct involvement of Stat-3 and Nanog in miR-21 gene upregulation, both Stat-3 and Nanog were first downregulated by Stat-3 siRNA or Nanog siRNA, respectively followed by the miR-21 promoter-specific ChIP assay as described above. Our results indicate that transfection of HNSCC cells with Nanog siRNAs (Fig. 3A-a,b,c, lane 6) or Stat-3 siRNA (Fig. 3A-a,b,c, lane 7), but not scrambled sequenced siRNA (Fig. 3A-a,b,c, lane 4 vs. lane 5) effectively blocks HA-mediated Nanog/Stat-3 binding to the miR-21 upstream/enhancer promoter region in HNSCC cells. Identical amplification products were detected in the positive controls from total input chromatin (Fig. 3A-e, lane 1–7). Moreover, no amplification was seen in samples that were processed in IgG isotype control-mediated precipitation (Fig. 3A-d, lane 1–7). We observed similar results by quantitative RT-PCR (data not shown). Thus, these results verify that Nanog-associated Stat-3 binds directly (or forms as part of the complex) to the promoter region of miR-21 in HSC-3 cells following HA-CD44 interaction.

In order to establish the specificity of the Stat-3/Nanog siRNAs used in this study, HSC-3 cells were transfected with siRNA sequences targeting human Nanog or Stat-3 followed by immunoblotting with anti-Stat-3 antibody or anti-Nanog antibody, respectively. Our results clearly indicate that Stat-3 siRNA target sequences successfully suppress the expression of Stat-3 (but not Nanog) in HNSCC cells (Fig. 3B-a,b,c), whereas Nanog siRNA target sequences effectively block Nanog (but not Stat-3) expression in HNSCC cells (Fig. 3B-a,b,c). In control samples, neither Stat-3 nor Nanog is downregulated in HSC-3 cells treated with transfection reagents containing scrambled siRNA (Fig. 3B-a,b,c). Therefore, we conclude that the downregulation of Stat-3 or Nanog expression by either Stat-3 siRNA or Nanog siRNA used in our study is specific.

(2) Production of miR-21 in HNSCC cells—The expression of mature-miR-21 has been shown to be involved in HNSCC progression (Chang, et al., 2008; Volinia, et al., 2006). To determine whether miR-21 levels are increased following the binding of HA to CD44, we first prepared small RNAs followed by an RNase protection assay using the miRNA Detection Kit (Ambion). Our results indicate that the level of miR-21 is increased in HSC-3 cells treated with scrambled sequence siRNA plus HA (Fig. 4a-lane 2) compared with those cells without HA treatment (Fig. 4a-lane 1). HSC-3 cells treated with Nanog siRNA (Fig. 4a-lane 4) or Stat-3 siRNA (Fig. 4a-lane 5) show significantly less HA-induced miR-21 expression. These findings support the notion that both Nanog and Sta-3 are required for miR-21 production in HA-activated HNSCC cells. We also noted that the increase of miR-21 expression was specifically a result of the interaction between HA and CD44 since pretreatment of HSC-3 cells with anti-CD44 antibody plus HA addition significantly reduces miR-21 production (Fig. 4a-lane 3). Moreover, we have found that the expression of miR-21 can be induced in cells treated with a miRNA-negative control upon addition of HA (Fig. 4a-lane 7 vs. lane 6). In contrast, the treatment of HSC-3 cells with an anti-miR-21 inhibitor plus HA results in a decrease in miR-21 expression (Fig. 4a-lane 8). We believe that these changes in miR-21 expression under various treatment conditions was not due to the variations of RNA extracted from each sample since there were very similar levels of the miR-191 control in all samples (Fig. 4b-lane 1–8). Together, these findings

strongly suggest that HA/CD44-activated Nanog and Stat-3 signaling plays an important role in the production of miR-21 in HNSCC cells.

The impact of HA/CD44-mediated miR-21 (induced by Nanog and Stat-3 signaling) in PDCD4/IAP expression, anti-apoptosis and chemoresistance in HSC-3 cells

PDCD4 was identified as one of the tumor suppressor genes induced by miR-21 (Asangani, et al., 2008). Inhibitors of the apoptosis family of proteins (IAPs) [e.g., cIAP-1, cIAP-2 and X-linked IAPs (XIAP)] are frequently overexpressed by cancer cells. Importantly, upregulation of IAPs (c-IAP-1, c-IAP-2 and XIAP) is linked to chemoresistance by their binding to caspases and suppressing apoptosis (Hunter, 2007). Here, we demonstrate that basal levels of PDCD4 expression and IAPs were detected in cells treated with scrambled sequence siRNA without HA addition (Fig. 5a, lane 1; Fig. 5b-d, lane 1) or pretreated with anti-CD44 antibody followed by HA addition (Fig. 5a, lane 3; Fig. 5b-d, lane 3). In contrast, PDCD4 expression was significantly reduced and IAPs are greatly enhanced in cells treated with scrambled sequence siRNA in the presence of HA (Fig. 5a, lane 2; Fig. 5b-d, lane 2). Further analyses indicate that HSC-3 cells treated with Nanog siRNA or Stat-3 siRNA (in the presence of HA) displays an elevated level of PDCD4 expression (Fig. 5a, lane 4 and lane 5) and a decreased amount of XIAP expression (Fig. 5b-d, lane 4 and lane 5). These observations confirm that HA/CD44-mediated Nanog and Stat-3 signaling is closely linked to the expression of PDCD4 and/or IAPs in HSC-3 cells. We also noted that downregulation of miR-21 by treating HSC-3 cells with an anti-miR-21 inhibitor (but not a negative-control miRNA) promotes upregulation of PDCD4 expression (Fig. 5a, lane 8 vs. lane 6 and lane 7) and downregulation of IAPs (Fig. 5b-d, lane 8 vs. lane 6 and lane 7) in the presence of HA. These results indicate that the signaling network consisting of Nanog, Stat-3 and miR-21 is functionally coupled with the inhibition of the tumor suppressor protein (PDCD4) expression and the stimulation of survival protein (e.g., XIAP) production. These specific effects may facilitate the progression of HA/CD44-activated HNSCC cells.

Further analyses indicate that the addition of HA enhances cell growth/survival and reduces apoptosis in untreated control cells or anti-CD44 antibody treated cells (i.e., without chemotherapeutic drugs) and decreases the ability of cisplatin to induce tumor apoptosis and cell death (Table 1A). These observations strongly suggest that HA causes both a decrease in apoptosis and an increase in tumor cell growth and survival (Table 1A) leading to the enhancement of chemoresistance (Table 1A). Moreover, downregulation of Nanog, Stat-3 or miR-21 [by treating HSC-3 cells with Nanog siRNA or Stat-3 siRNA or transfected HSC-3 cells with an anti-miR-21 inhibitor (but not scrambled sequence siRNA or with miRNA-negative control)] effectively attenuates HA-mediated tumor cell growth/anti-apoptosis/survival and enhances multi-drug sensitivity in HSC-3 cells (Table 1A). These findings suggest that the HA/CD44-mediated Nanog/Stat-3 signaling pathways and miR-21 function may represent new targets to cause tumor cells to undergo apoptosis/death and overcome chemotherapy resistance in head and neck cancer cells.

Apparently, both PDCD4 loss and IAP protein gain are responsible for HA-mediated cisplatin resistance in HNSCC cells (Fig. 5). Recently, a small molecule IAP protein inhibitor (bivalent SM-164) has been shown concurrently target cIAP-1/cIAP-2 for

degradation and antagonize XIAP leading to an enhancement of tumor cell apoptosis and tumor regression (Lu, et al. 2008). In this study, we have found that chemosensitivity increases with a newly developed IAP protein inhibitor, SM164 (Table 1B). These findings suggest that the use of a combination of IAP protein inhibitor (SM164) and cisplatin may improve the efficacy of chemotherapeutic drug treatments for head and neck cancer.

DISCUSSION

The primary tumor type in head and neck cancer is squamous cell carcinoma (HNSCC). These tumor cells display persistent cell growth leading to chemoresistance and recurrence (Parkin, et al., 2005). Hyaluronan (HA), the major glycosaminoglycan found in the extracellular matrix of mammalian tissues, is now considered to be a physiologically-relevant ligand for CD44 (also known as a hyaluronan receptor) in many cell types including HNSCC cells (Wang and Bourguignon, 2011). Most of malignant solid tumors display high levels of both HA and CD44 (Toole and Hascall, 2002; Toole, et al., 2002; Wang and Bourguignon, 2009). HA-CD44 interaction has been shown to promote oncogenic signaling and tumor cell-specific properties (Turley, et al., 2002; Bourguignon, 2008). In this study we focused on determining which oncogenic pathways are directly involved in regulating HA and CD44-specific HNSCC cell behaviors such as chemotherapy resistance.

Nanog has been suggested as one of the major factors that render the reprogramming adult stems into germ-line-competent induced pluripotent stem (iPS) cells (Kashyap, et al., 2009). It is expressed not only in germ cell tumors, but also found to be expressed in many other tumors including HNSCC cells and tissues (Chiou, et al., 2008). In this study we also detected Nanog expression in HNSCC cells (e.g., HSC-3 cells) (Figs. 1 and 2). The fact that Nanog overexpression is closely associated with HNSCC cells and tissues suggests that its expression may be implicated in self-renewal and tumorigenesis via activating its downstream target genes. The question of how Nanog signaling pathway plays a role in regulating HNSCC cell activation has not been well-understood.

Overexpression miR-21 is detected in various HNSCC cell lines and patient specimens (Volinia, et al., 2006; Chang, et al., 2008). Accumulating evidence indicates that miR-21 is closely associated with both cancer development and chemotherapy resistance (Bourguignon, et al., 2009a). Nanog appears to be involved in the regulation of pri-miRNA expression during cancer development (Bourguignon, et al., 2009a). Our previous work showed that HA/CD44-activated PKC ϵ promotes Nanog interaction with p68 and DROSHA leading to biosynthetic processing and production of miR-21 in breast tumor cells (Bourguignon, et al., 2009). These findings suggest that HA/CD44-mediated Nanog signaling is closely linked to miR-21 production and function during oncogenesis.

Abnormal Stat-3 signaling appears to play a critical role in oncogenesis (Huang, 2007). In particular, constitutive activation of Stat-3 such as tyrosine phosphorylated Stat-3 has been observed in human malignancies including HNSCC (Huang, 2007). Previous studies showed that the functional link between Nanog and Stat-3 exists in several different tumor cells (Bourguignon, et al., 2008). In this study we observed that HA-CD44 binding activates Nanog/Stat-3 (also tyrosine phosphorylated Stat-3) nuclear localization and complex

formation in HSC-3 cells (Figs. 1–3). Thus, identifying specific genes that are transcriptionally controlled by the Nanog-Stat-3 interaction in the nucleus may be very important for the understanding of the disease mechanism occurring during HNSCC progression. Activation of Stat-3 has also been shown to up-regulate the mRNA levels of many genes, including *miR-21* (Löffler D, 2007).

Here, we have provided new evidence that HA/CD44 activates Nanog-Stat-3 (also p-Stat-3) complex formation and nuclear translocation in HNSCC cells (Figs. 1 and 2). Our results also indicate that miR-21 is controlled by an upstream promoter/enhancer containing Stat-3 binding sites in HNSCC cells, while chromatin immunoprecipitation (ChIP) assays demonstrate that stimulation of miR-21 production by HA is Nanog/Stat-3 complex-dependent in HNSCC cells (Fig. 3). Most importantly, an anti-miR-21 inhibitor can enhance PDCD4 expression (Fig. 5), and block HA/CD44-mediated tumor functions [e.g., survival protein expression (Fig. 5), tumor cell growth and survival/chemotherapy resistance (Table 1)] in HNSCC cells. Thus, this newly-discovered HA/CD44-Nanog/Stat-3 signaling pathway and miR-21 production/function are highly innovative and should provide important new drug targets to cause tumor cell apoptosis and overcome chemotherapy resistance in head and neck cancer cells.

Cisplatin is the most common anti-head and neck chemotherapy used today. The ability of this drug to induce tumor cell death is often counteracted by the presence of anti-apoptotic regulators leading to chemoresistance (Nakamura, et al., 2005; Torre, et al., 2010; Wang and Bourguignon, 2011). Several lines of evidence point toward the IAP family (e.g., c-IAP-1, c-IAP-2 and XIAP) playing a role in oncogenesis via their effective suppression of apoptosis (Hunter, 2007). The mode of action of IAPs in suppressing apoptosis appears to be through direct inhibition of caspases and pro-caspases (primarily caspase 3 and 7) (Hunter, 2007). IAPs also support chemoresistance by preventing tumor cell death induced by anticancer agents (Gyrd-Hansen and Meier, 2010). Although certain anti-apoptotic proteins (e.g., Bcl-xL) have been shown to participate in anti-apoptosis and chemoresistance in HA/CD44-activated breast tumor cells (Bourguignon, et al., 2009b), the involvement of IAPs in HA/CD44-mediated HNSCC cell survival and chemoresistance has not been fully elucidated.

In this study we demonstrated that HA/CD44-activated Nanog/Stat-3 signaling and miR-21 reduce PDCD4 expression (Fig. 5) resulting in oncogenesis [by enhancing the expression of inhibitors of anti-apoptosis proteins (IAPs) (Fig. 5)]. Furthermore, downregulation of HA/CD44-activated Nanog/Stat-3 signaling (by Nanog siRNA/Stat-3 siRNA) and miR-21 production (by anti-miR-21 inhibitor) not only induces PDCD4 upregulation (Fig. 5), but also inhibits the expression of survival proteins (e.g., c-IAP-1, c-IAP-2 and XIAP) (Fig. 5). Subsequently, these signaling perturbation events contribute to apoptosis and chemosensitivity (Table 1). Our preliminary data indicate that (i) PDCD4 downregulation can be detected as early as 30–60 min after HA binding to CD44, whereas IAP protein upregulation can be detected 5–6 hours after HA-CD44 interaction; and (ii) PDCD4 overexpression blocks IAP protein expression. After 24h HA addition, a maximal level of PDCD4 loss and IAP overexpression can be reached in HNSCC cells. Therefore, this time point was used in Fig. 5. However, the cellular and molecular mechanisms involved in the regulation of these causal links between Nanog/Stat-3 signaling and miR-21 function

including PDCD4 downregulation, IAP upregulation, anti-apoptosis and chemoresistance will need to be resolved by further experiments.

As summarized in Fig. 6, we propose that HA binding (Step 1) promotes CD44 association with Nanog and Stat-3 (also tyrosine phosphorylated Stat-3, p-Stat-3) (step 2). Nanog and Stat-3 (also p-Stat-3) then translocate from the cytosol to the nucleus and interacts with an upstream/enhancer region (containing Stat-3 binding sites) of the miR-21 promoter (step 4), resulting in miR-21 gene expression and mature miR-21 production (step 5). The resultant miR-21 then functions to downregulate the tumor suppressor protein (PDCD4) (step 6a) and promotes HNSCC cell activation (step 7a) leading to IAP (c-IAP-1, c-IAP-2 and XIAP) expression, HNSCC cell anti-apoptosis/survival and chemoresistance. In direct contrast, treatment of HNSCC cells with an anti-miR-21 inhibitor induces tumor suppressor protein (PDCD4) upregulation (step 6b). Subsequently, these changes result in the inhibition of IAP (c-IAP-1, c-IAP-2 and XIAP) expression (Fig. 7b), stimulation of apoptosis and enhancement of chemosensitivity in HNSCC cells. Taken together, these findings suggest that targeting HA/CD44-mediated Nanog-Stat-3 signaling pathways and miR-21 function may provide a new drug target to sensitize tumor cell apoptosis/death and overcome chemotherapy resistance in HNSCC cells.

MATERIALS AND METHODS

Cell Culture

The cell line, HSC-3 cells (Japan Cancer Research Resources Bank, Tokyo), was established in 1985 from a primary oral squamous cell carcinoma removed from the tongue of a 64-year-old male patient. The HSC-3 cells were maintained in Dulbecco Modified Eagle medium supplemented with 10% fetal bovine serum. Cells were routinely serum starved (and therefore deprived of serum HA) before adding HA.

Antibodies and Reagents

Monoclonal rat anti-CD44 antibody (Clone: 020; Isotype: IgG_{2b}; obtained from CMB-TECH, Inc., San Francisco, CA.) recognizes a determinant of the HA-binding region common to CD44 and its principal variant isoforms. This rat anti-CD44 was routinely used for HA-related blocking experiments and immunoprecipitation. Immuno-reagents such as rabbit anti-Stat-3 antibody, goat anti-Nanog antibody, mouse anti-PDCD4 antibody, and goat anti-actin antibody were purchased from Santa Cruz Biotechnology, Inc. (Santa Cruz, CA). Mouse anti-c-IAP-1 antibody, mouse anti-c-IAP-2 and mouse anti-XIAP antibody were from BD (Franklin Lakes, NJ). Rabbit anti-phospho-Stat-3 (pY[705], tyrosine 705 residue) was from Cellular Signaling Technology (Beverly, MA). Cisplatin, was obtained from Sigma Chemicals (St. Louis, MO). Healon HA polymers (~500,000dalton polymers), purchased from Pharmacia & Upjohn Company (Kalamazoo, MI) was prepared by gel filtration chromatography using a Sephacryl S1000 column (GE Healthcare Biosciences).

Anti-miR-21 Inhibitor Preparation and Transfection

Anti-miRTM targeting miR-21 (anti-miR-21 inhibitor) (Ambion, catalog number, 17000) and its corresponding negative control (Ambion, catalog number, 17010) were transfected into

HSC-3 cells using Lipofectamine 2000 reagent (Invitrogen) for 24h. Cells were then treated with HA or without HA in various experiments as described below. The final concentrations of anti-miR-21 inhibitor and miRNA-negative control used in various experiments were 30nmol/L.

Immunoprecipitation and Immunoblotting Techniques

Immunoprecipitation was conducted after homogenization of the cell lysate using rat anti-CD44 antibody followed by goat anti-rat IgG-beads. Subsequently, the immunoprecipitated materials were immunoblotted with rabbit anti-Nanog antibody (2µg/ml) or rabbit anti-Stat-3 antibody (2µg/ml) or rabbit anti-phospho-Stat-3 (pY[705]) (2µg/ml). The nuclear fraction [using the extraction kit from Active Motif (Carlsbad, CA)] of HSC-3 cells (untreated or pretreated with anti-CD44 antibody) plus 50µg/ml HA (or no HA) for various time intervals (e.g. 0, 5min, 15min or 60min) at 37°C] was also used for goat anti-Nanog antibody-conjugated immunoprecipitation followed by rabbit anti-Stat-3-mediated immunoblot, respectively.

In some cases, cell lysate of HSC-3 cells [pretreated with anti-CD44 antibody or transfected with Nanog siRNA or Stat-3 siRNA or siRNA with scrambled sequences; or anti-miR-21 inhibitor or miRNA-negative control or without any treatment) followed by HA (50µg/ml) addition (or no HA addition) for various time intervals (e.g. 0, 5min, 10min, 15min, 30min, 60min or 24h) at 37°C] were also immunoblotted using various immuno-reagents [e.g., mouse anti-PDCD4 (2µg/ml) or mouse anti-c-IAP-1 or mouse anti-c-IAP-2 antibody and anti-XIAP (2µg/ml) or goat anti-actin (2µg/ml) (as a loading control), respectively].

Chromatin Immunoprecipitation (ChIP) Assay

To examine whether Nanog-Stat-3 complex directly interacts with the upstream promoter/enhancer region of miR-21, chromatin immunoprecipitation (ChIP) assays was performed in HNSCC cells [pretreated with anti-CD44 antibody or transfected with Nanog siRNA or Stat-3 siRNA or siRNA with scrambled sequences] treated with HA (50µg/ml) or without HA using a kit (EZ ChIP) from Millipore Corp according to the manufacturer's instructions. Cross-linked chromatin lysates were sonicated and diluted with ChIP sonication buffer plus protease inhibitors, divided and incubated with normal rabbit IgG or rabbit anti-Nanog antibody or rabbit anti-Stat-3 antibody or rabbit anti-phospho-Stat-3 (pY[705]) antibody at 4°C overnight, then precipitated with protein G-agarose. Cross-linking was reversed by overnight 65°C incubation; DNA fragments were then extracted with PCR purification kit, analyzed by PCR and quantitated by real-time PCR using primer pairs specific for the miR-21 upstream promoter/enhancer region containing the Stat-3 binding sites: forward primer: 5'-CTGGGAGAAACCAAGAGCTG-3' and reverse primer: AGGGGACAAGTCAGAGAGAGG-3' on an agarose gel as described previously (Löffler, et al., 2007).

RNase Protection Assay Analysis of Mature miRNAs

Expression of miRNAs was qualitatively analyzed by RNase protection assay. For RNase protection assay, enriched small RNA isolated from HSC-3 cells [transfected with scrambled sequence siRNA with (or without) anti-CD44 antibody or transfected with Nanog

siRNA or Stat-3 siRNA or siRNA or anti-miR-21 inhibitor or miRNA-negative control in the presence or absence of HA for various time intervals (e.g., 0, 5min, 10min, 15min, 30min or 2h) at 37°C] was enriched and purified using the *mirVana* miRNA Isolation kit (Ambion). RNA concentrations were verified by measuring absorbance (A_{260}) on the NanoDrop Spectrophotometer ND-1000 (NanoDrop). The *mirVana* miRNA probe construction kit (Ambion) was used to synthesize the ^{32}P -labeled miR-21 antisense probe and miR-191 probe loading control as described previously (Bourguignon, et al., 2009a).

Immunofluorescence Staining

HSC-3 cells (untreated or pretreated with anti-CD44 antibody) were incubated with HA (50µg/ml) at 37°C for various time intervals (e.g., 0, 10, 30 or 60min) or with no HA. These cells were then fixed with 2% paraformaldehyde. Subsequently, these cells were rendered permeable by ethanol treatment followed by incubating with Texas Red-conjugated anti-Nanog antibody and fluorescein (FITC)-conjugated anti-Stat-3 antibody followed by DAPI staining (a marker for nucleus). To detect non-specific antibody binding, DAPI-labeled cells were incubated with FITC or Texas Red-conjugated normal IgG, respectively. No labeling was observed in control samples. These fluorescence-labeled samples were then examined with a confocal laser scanning microscope.

Clinical Tumor Samples

IRB approval was obtained from our institution's Committee on Human Research. The clinical tissue specimens were portions of primary tumors of patients undergoing surgical treatment of head and neck squamous cell carcinomas (HNSCC) from multiple primary sites of the upper aerodigestive tract at a UCSF university-affiliated Veterans Affairs Medical Center from September 1, 2001 to June 30, 2006. The presence of 80% cancer cells in the procured samples was confirmed by a clinical pathologist as described previously (Wang et al., 2009).

Immunohistochemistry

The tissue specimens were fixed in 4% paraformaldehyde in 0.1 M phosphate buffer for 24 hours at 4°C and embedded in paraffin. Five µm-thick tissue sections were placed on positively charged glass slides (Fisher Scientific, Pittsburgh, PA, USA). Immunohistochemical stains were performed using the Vectastain ABC kit (Vector Laboratories, Burlingame, CA, USA), according to the manufacturer's protocol. Rabbit anti-Nanog antibody or rabbit anti-Stat-3 antibody (dilution factor from 1:100 up to 1:1000 determined by titration) were applied to tissue sections and incubated overnight at 4°C. Secondary biotinylated antibody and streptavidin-HRP conjugate complex were applied for 60 and 30 minutes, respectively. After washing in buffer, the chromogen diaminobenzidine was applied for 5 minutes followed by a counterstain with Mayer's hematoxylin. Negative controls included substituting the primary antisera with preimmune sera from the same species and omitting the primary antibody, or by using an antibody of irrelevant specificity. In some cases, these clinical samples were also incubated with Texas Red-conjugated anti-Nanog antibody and fluorescein (FITC)-conjugated anti-Stat-3 antibody or rabbit anti-phospho-Stat-3 (pY[705] antibody, respectively. To detect non-specific antibody binding,

HNSCC tumor sections were also incubated with FITC or Texas Red-conjugated normal IgG, respectively. No labeling was observed in control samples. These fluorescence-labeled samples were then examined with a confocal laser scanning microscope.

Tumor Cell Growth and Apoptosis Assays

HSC-3 cells were transfected with either scrambled sequence siRNA or with Nanog siRNA (or Stat-3 siRNA) or anti-miR-21 inhibitor or miRNA-negative control or pretreated with anti-CD44 antibody, as above. Some cells were also treated with an IAP inhibitor, SM164 (2nM) or vehicle control. These cells (5×10^3 cells/well) were then incubated with various concentrations of cisplatin (4×10^{-9} M - 1.75×10^{-5} M) with no HA or with HA (50ug/ml). After 24h incubation at 37°C, MTT-based growth assays were analyzed as described previously (Bourguignon, 2008, 2009a, 2009b). The percentage of absorbance relative to untreated controls (i.e., cells treated with neither HA nor chemotherapeutic drugs) was plotted as a linear function of drug concentration. The 50% inhibitory concentration (IC₅₀) was identified as a concentration of drug required to achieve a 50% growth inhibition relative to untreated controls. For apoptosis assay, FITC-conjugated Annexin V (for measuring apoptotic cells) using Apoptosis Detection Kit (Calbiochem, San Diego, CA) was used according to the manufacturer's protocol (Bourguignon, et al., 2009b).

Acknowledgments

We gratefully acknowledge the assistance of Drs. Gerard J. Bourguignon and Walter M. Holleran in the preparation and review of this manuscript. We are grateful for Ms. Christina Camacho for her assistance in preparing graphs and illustrations. We would also like to thank for Dr. Shaomeng Wang from the University of Michigan for providing us an IAP inhibitor, SM164. This work was supported by Veterans Affairs (VA) Merit Review grant and United States Public Health grants (R01 CA66163, R01 CA78633 and P01 AR39448). L.Y.W.B is a VA Senior Research Career Scientist.

References

- Asangani IA, Rasheed SAK, Nikolova DA, Leupold JH, Colburn NH, Post S, et al. Allgayer H. MicroRNA-21 (miR-21) post-transcriptionally downregulates tumor suppressor Pcd4 and stimulates invasion, intravasation and metastasis in colorectal cancer. *Oncogene*. 2008; 27:2128–2136. [PubMed: 17968323]
- Bourguignon LY. Hyaluronan-mediated CD44 activation of RhoGTPase signaling and cytoskeleton function promotes tumor progression. *Semin Cancer Biol*. 2008; 18:251–259. [PubMed: 18450475]
- Bourguignon LY, Peyrollier K, Xia W, Gilad E. Hyaluronan-CD44 interaction activates stem cell marker Nanog, Stat-3-mediated MDR1 gene expression, and ankyrin-regulated multidrug efflux in breast and ovarian tumor cells. *J Biol Chem*. 2008; 283:17635–17651. [PubMed: 18441325]
- Bourguignon LY, Spevak CC, Wong G, Xia W, Gilad E. Hyaluronan-CD44 interaction with PKC ϵ promotes oncogenic signaling by the stem cell marker, Nanog and the production of microRNA-21 leading to downregulation of the tumor suppressor protein, PDCD4, anti-apoptosis and chemotherapy resistance in breast tumor cells. *J Biol Chem*. 2009a; 284:26533–26546. [PubMed: 19633292]
- Bourguignon LY, Xia W, Wong G. Hyaluronan-mediated CD44 interaction with p300 and SIRT1 regulates beta-catenin signaling and NF κ B-specific transcription activity leading to MDR1 and Bcl-xL gene expression and chemoresistance in breast tumor cells. *J Biol Chem*. 2009b; 284:2657–2671. [PubMed: 19047049]
- Bourguignon LY, Wong G, Earle C, Krueger K, Spevak CC. Hyaluronan-CD44 interaction promotes c-Src-mediated Twist signaling, microRNA-10b expression and RhoA/RhoC upregulation leading

to Rho-Kinase-associated cytoskeleton activation and breast tumor cell invasion. *J Biol Chem.* 2010; 285:36721–36735. [PubMed: 20843787]

Chang SS, Jiang WW, Smith I, Poeta LM, Begum S, Glazer C, et al. MicroRNA alterations in head and neck squamous cell carcinoma. *Int J Cancer.* 2008; 123:2791–2797. [PubMed: 18798260]

Chiou SH, Yu CC, Huang CY, Lin SC, Liu CJ, Tsai TH. Positive correlations of Oct-4 and Nanog in oral cancer stem-like cells and high-grade oral squamous cell carcinoma. *Clin Cancer Res.* 2008; 14:4085–4095. [PubMed: 18593985]

Darnell JE Jr. STATs and gene regulation. *Science.* 1997; 277:1630–1635. [PubMed: 9287210]

Ezeh UI, Turek PJ, Reijo RA, Clark AT. Human embryonic stem cell genes OCT4, NANOG, STELLAR, and GDF3 are expressed in both seminoma and breast carcinoma. *Cancer.* 2005; 104:2255–2265. [PubMed: 16228988]

Gyrd-Hansen M, Meier P. IAPs: from caspase inhibitors to modulators of NF-kappaB, inflammation and cancer. *Nat Rev Cancer.* 2010; 10:561–574. [PubMed: 20651737]

Heinrich PC, Behrmann I, Haan S, Hermanns HM, Muller-Newen G, Schaper F. Principles of interleukin (IL)-6-type cytokine signalling and its regulation. *Biochem J.* 2003; 374:1–20. [PubMed: 12773095]

Huang S. Regulation of metastases by signal transducer and activator of transcription 3 signaling pathway: clinical implications. *Clin Cancer Res.* 2007; 13:1362–1366. [PubMed: 17332277]

Hunter AM. The inhibitors of apoptosis (IAPs) as cancer targets. *Apoptosis.* 2007; 12:1543–1568. [PubMed: 17573556]

Jemal A, Siegel R, Ward E, Hao Y, Xu J, Murray T, et al. Cancer statistics, 2008. *CA Cancer J Clin.* 2008; 58:71–96. [PubMed: 18287387]

Kashyap V, Rezende NC, Scotland KB, Shaffer SM, Persson JL, Gudas LJ, et al. Regulation of stem cell pluripotency and differentiation involves a mutual regulatory circuit of the NANOG, OCT4, and SOX2 pluripotency transcription factors with polycomb repressive complexes and stem cell microRNAs. *Stem Cells Dev.* 2009; 18:1093–1108. [PubMed: 19480567]

Löffler D, Brocke-Heidrich K, Pfeifer G, Stocsits C, Hackermüller J, Kretzschmar AK, et al. Interleukin-6 dependent survival of multiple myeloma cells involves the Stat3-mediated induction of microRNA-21 through a highly conserved enhancer. *Blood.* 2007; 110:1330–1333. [PubMed: 17496199]

Lu J, Bai L, Sun H, Nikolovska-Coleska Z, McEachern D, Qiu S, Miller RS, Yi H, Shangary S, Sun Y, Meagher JL, Stuckey JA, Wang S. SM-164: a novel, bivalent Smac mimetic that induces apoptosis and tumor regression by concurrent removal of the blockade of cIAP-1/2 and XIAP. *Cancer Res.* 2008; 68:9384–9393. [PubMed: 19010913]

Mitsui K, Tokuzawa Y, Itoh H, Segawa K, Murakami M, Takahashi K, et al. The homeoprotein Nanog is required for maintenance of pluripotency in mouse epiblast and ES cells. *Cell.* 2003; 113:631–642. [PubMed: 12787504]

Nakamura M, Nakatani K, Uzawa K, Ono K, Uesugi H, Ogawara K. Establishment and characterization of a cisplatin-resistant oral squamous cell carcinoma cell line, H-1R. *Oncol Rep.* 2005; 14:1281–1286. [PubMed: 16211297]

Parkin DM, Bray F, Ferlay J, Pisani P. Global cancer statistics, 2002. *CA Cancer J Clin.* 2005; 55:74–108. [PubMed: 15761078]

Song JI, Grandis JR. STAT signaling in head and neck cancer. *Oncogene.* 2000; 19:2489–2495. [PubMed: 10851047]

Toole BP, Hascall VC. Hyaluronan and tumor growth. *Am J Pathol.* 2002; 161:745–747. [PubMed: 12213700]

Toole BP, Wight TN, Tammi MJ. Hyaluronan-cell interactions in cancer and vascular disease. *J Biol Chem.* 2002; 277:4593–4596. [PubMed: 11717318]

Torre C, Wang SJ, Xia W, Bourguignon LY. Reduction of hyaluronan-CD44-mediated growth, migration, and cisplatin resistance in head and neck cancer due to inhibition of Rho kinase and PI-3 kinase signaling. *Arch Otolaryngol Head Neck Surg.* 2010; 136:493–501. [PubMed: 20479382]

Turley EA, Noble PW, Bourguignon LY. Signaling properties of hyaluronan receptors. *J Biol Chem.* 2002; 277:4589–4592. [PubMed: 11717317]

- Volinia S, Calin GA, Liu CG, Ambs S, Cimmino A, Petrocca F, Visone R, Iorio M, Roldo C, Ferracin M, Prueitt RL, Yanaihara N, Lanza G, Scarpa A, Vecchione A, Negrini M, Harris CC, Croce CM. A microRNA expression signature of human solid tumors defines cancer gene targets. *Proc Natl Acad Sci U S A*. 2006; 103:2257–2261. [PubMed: 16461460]
- Wang S, Bourguignon LY. Role of hyaluronan-mediated CD44 signaling in head and neck squamous cell carcinoma progression and chemoresistance. *Am J Pathol*. 2011; 178:956–963. [PubMed: 21356346]
- Wang SJ, Wong G, de Heer AM, Xia W, Bourguignon LY. CD44 variant isoforms in head and neck squamous cell carcinoma progression. *Laryngoscope*. 2009; 119:1518–1530. [PubMed: 19507218]
- Wen Z, Zhong Z, Darnell JE Jr. Maximal activation of transcription by Stat1 and Stat3 requires both tyrosine and serine phosphorylation. *Cell*. 1995; 82:241–250. [PubMed: 7543024]

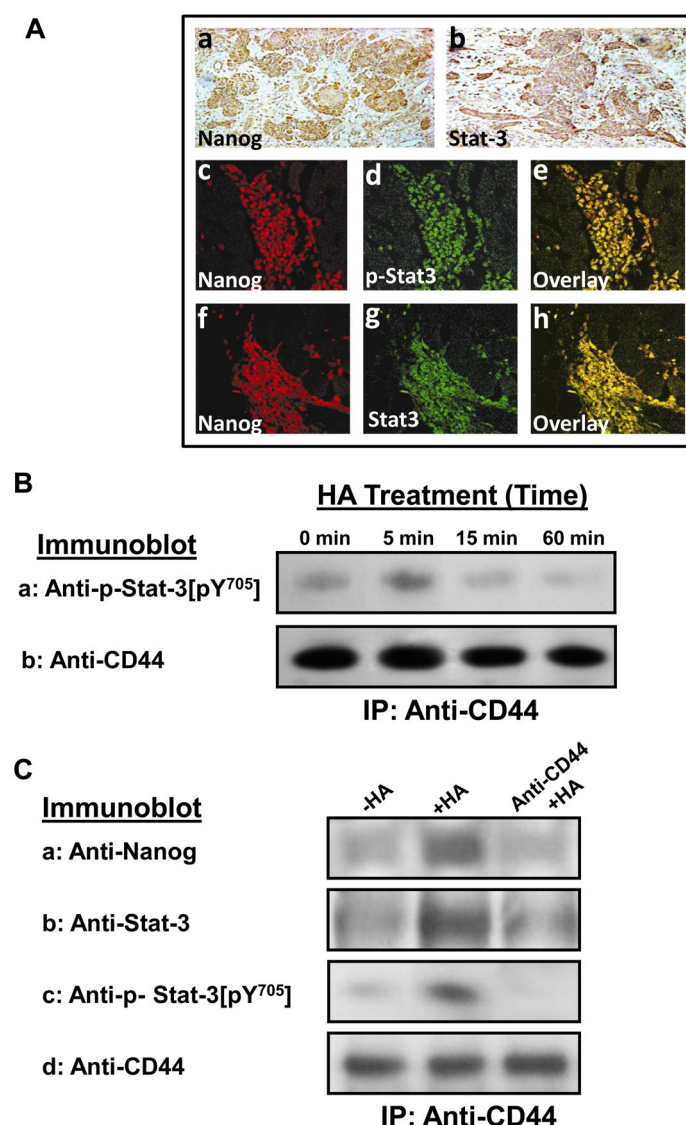


Fig. 1. Analyses of Nanog and Stat-3 expression in HNSCC patient samples and HSC-3 cells

A: Detection of Nanog and Stat-3 expression in head and neck squamous cell carcinoma (HNSCC) primary tumors. A panel of immune-reagents including rabbit anti-Nanog antibody, rabbit anti-Stat-3 antibody or rabbit anti-phospho-Stat-3 (pY[705]) antibody were used to examine the expression of both Nanog and Stat-3 in HNSCC primary tumors using immuno-peroxidase staining (a and b) or co-localization of Nanog with phosphorylated Stat-3 (p-Stat-3) (c-e) and total stat-3 (f-h) using double immunofluorescence staining as described in the Materials and Methods.

B: Time course analyses of HA/CD44-induced Stat-3 tyrosine phosphorylation: Cell lysates were prepared from HSC-3 treated with HA (50μg/ml) for various time intervals (e.g., 0, 5, 10, 15 and 60min) followed by anti-CD44-immunoprecipitation followed by immunoblotting with anti-phospho-Stat-3 [pY⁷⁰⁵] antibody or anti-CD44 antibody (as a loading control).

C: Detection of Nanog and Stat-3 (or phosphorylated Stat-3) in the CD44 complex by anti-CD44-immunoprecipitation followed by immunoblotting with anti-Nanog antibody (a) or anti-Stat-3 antibody (b) or anti-phospho-Stat-3 [pY⁷⁰⁵] antibody (c) or reblotting with anti-CD44 (d) as a loading control using HSC-3 cells treated with no HA or with HA (50µg/ml) for 5min or pretreated with anti-CD44 antibody for 1h followed by 5min HA (50µg/ml) addition.

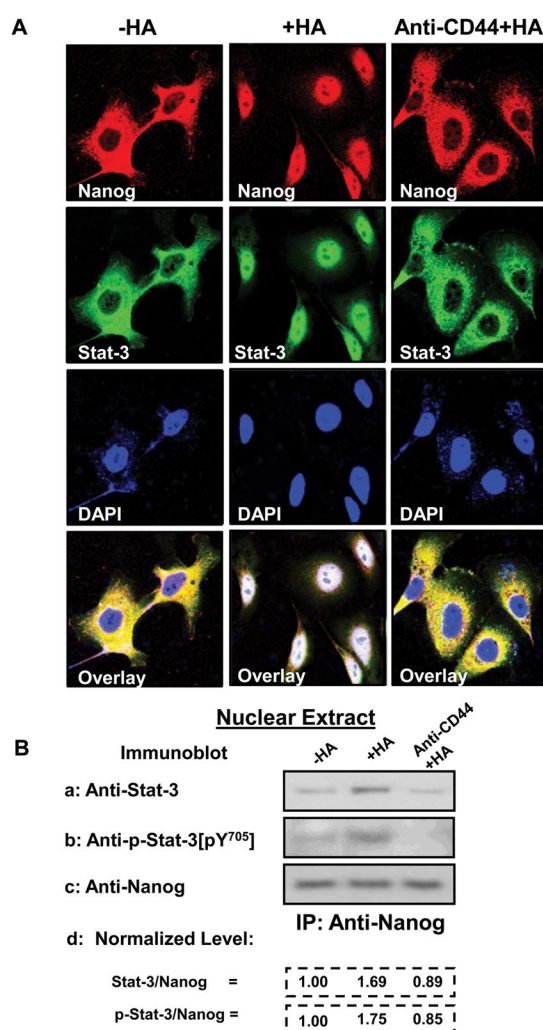


Fig. 2. Immunocytochemical and biochemical analyses of HA/CD44-induced Nanog and Stat-3 nuclear translocation in HSC-3 cells

A: Immunostaining of Nanog [using Texas Red-labeled anti-Nanog (red color) and Stat-3 using FITC-labeled anti-Stat-3 (green color)]: HSC-3 cells (untreated or pretreated with anti-CD44 antibody for 1h) were incubated with HA (50µg/ml) (or without HA) for 15min at 37°C and fixed by 2% paraformaldehyde. Subsequently, these cells were rendered permeable by ethanol treatment and immuno-stained with Texas Red-labeled anti-Nanog (red color) or FITC-labeled anti-Stat-3 (green color) and DAPI (a nuclear marker) (c) as described in the Materials and Methods. **B:** Analyses of HA/CD44-induced Nanog and Stat-3 complex formation in the nuclear fraction: HSC-3 cells (untreated or pretreated with anti-CD44 antibody for 1h) were incubated with HA (50µg/ml) (or without HA) for 15min at 37°C. Nuclear fractions of these cells were then prepared by anti-Nanog-immunoprecipitation followed by immunoblotting with anti-Stat-3 antibody (a) or anti-phospho-Stat-3 (pY⁷⁰⁵) (b) or reblotting with anti-Nanog (c) as a loading control as described in the Materials and Methods [untreated cells (-HA); cells treated with HA (+HA) for 15min; lane 3: cells pretreated with anti-CD44 antibody for 1h plus 15min HA addition (anti-CD44 +HA)].

[The ratio of Stat-3 or phosphorylated Stat-3 and Nanog (the loading control) (d) was determined by densitometry, and the levels were normalized to untreated (no HA treatment) value (designated as 1.00); the values expressed represent an average of triplicate determination of 3 experiments with an SD of less than 5%].

Author Manuscript

Author Manuscript

Author Manuscript

Author Manuscript

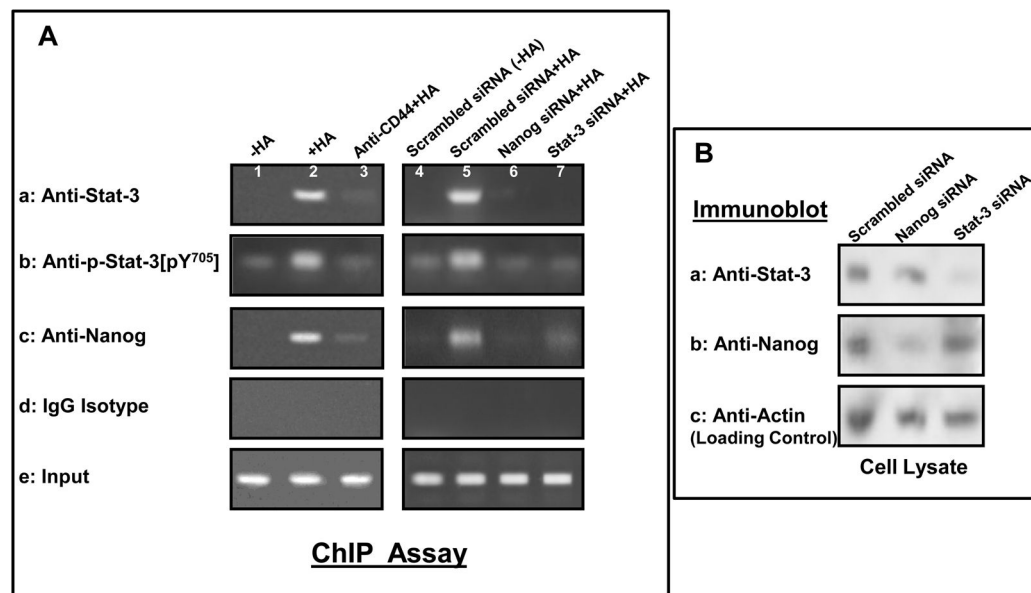
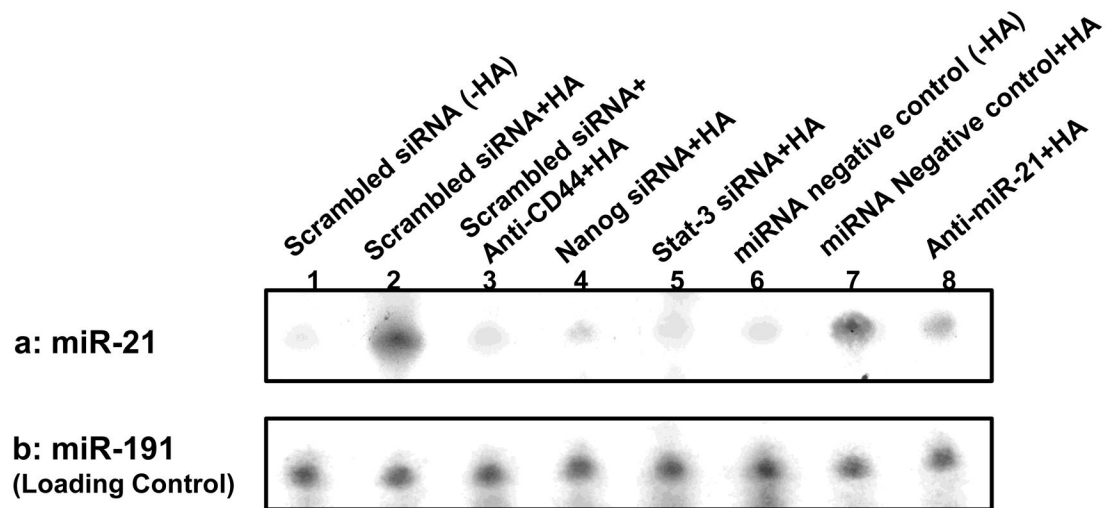


Fig. 3. Interaction between Nanog, Stat-3 and the upstream promoter/enhancer region of miR-21 promoter in HSC-3 cells

A: *In vivo* binding of Nanog and Stat-3 (or phosphorylated Stat-3) to the miR-21 upstream promoter/enhancer region in HSC-3 cells: ChIP assay was performed in HSC-3 cells following protocols described in the Materials and Methods using the Stat-3 binding site-containing miR-21 promoter (upstream promoter/enhancer region)-specific primers by PCR. Identical volumes from the final precipitated materials were used for the PCR reactions [untreated cells (lane 1); cells treated with HA for 30min (lane 2); cells pretreated with anti-CD44 antibody for 1h plus 30min HA addition (lane 3); cells pretreated with scrambled siRNA with no HA (lane 4); cells pretreated with scrambled siRNA plus 30min HA addition (lane 5); cells pretreated with Nanog siRNA plus 30min HA addition (lane 6); cells pretreated with Stat-3 siRNA plus 30min HA addition) (lane 7). (a: anti-Stat-3-mediated immunoprecipitated material; b: anti-phospho-Stat-3 (pY⁷⁰⁵)-mediated immunoprecipitated material; c: anti-Nanog-mediated immunoprecipitated material; d: IgG isotype control-mediated precipitated material; e: total input materials). **B:** Verification of the specificity of Nanog siRNA or Stat-3 siRNA used in the study.

Cell lysates isolated from HSC-3 cells [transfected with Nanog siRNA or Stat-3 siRNA-target or scrambled siRNA] were solubilized by 1% Nonidet P-40 (NP-40) buffer followed by immunoblotting with anti-Stat-3 antibody (a), anti-Nanog antibody (b) or anti-actin (a loading control) (c).



RNase Protection Assay

Fig. 4. Detection of HA/CD44-induced miR-21 production in HSC-3 cells

Detection of miR-21 in HSC-3 cells using RNase protection assay as described in the Materials and methods. A: Autoradiogram of miR-21 detected in HSC-3 cells incubated with scrambled sequence siRNA [without HA (lane 1) or with 2h HA treatment (lane 2) or pretreated with anti-CD44 antibody for 1h followed by HA addition for 2h (lane 3) or incubated with Nanog siRNA plus 2h HA treatment (lane 4) or incubated with Stat-3 siRNA plus 2h HA treatment (lane 5) or incubated with miRNA-negative control [without HA (lane 6) or with 2h HA treatment (lane 7)] or incubated with an anti-miR-21 inhibitor plus 2h HA treatment (lane 8). (Autoradiogram of miR-191 in each gel lane was used as a loading control).

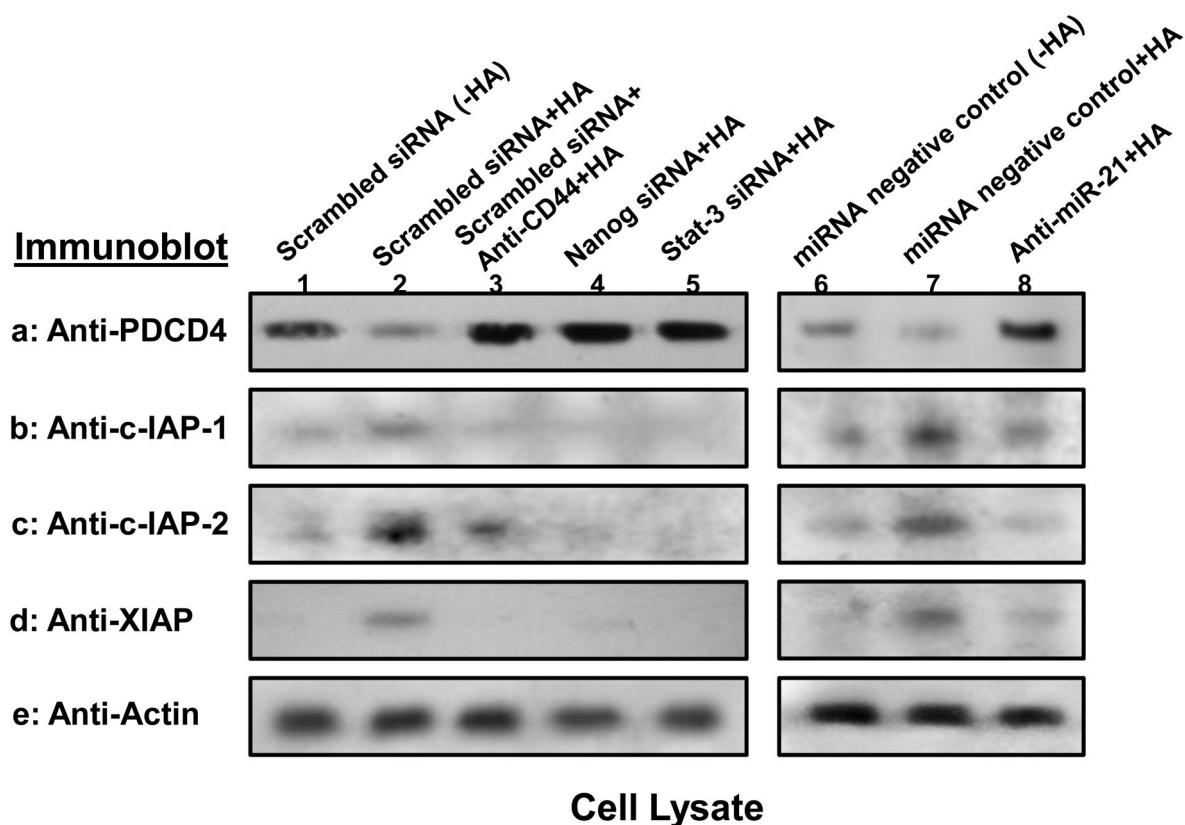


Fig. 5. Analyses of HA/CD44-mediated PDCD4 and IAP expression in HSC-3 cells

Detection of HA/CD44-induced PDCD4 and IAP (cIAP-1, cIAP-2 and XIAP) expression in HSC-3 cells was performed by solubilizing cells with 1% Nonidet P-40 (NP-40) buffer followed by immunoblotting with anti-PDCD4 antibody or anti-cIAP-1 antibody or anti-cIAP-2 antibody or anti-XIAP antibody, respectively as described in the Materials and Methods.

First, cell lysates were prepared from HSC-3 cells treated with scrambled sequence siRNA [without HA (lane 1) or with HA for 24h (lane 2)] or treated with anti-CD44 antibody for 1h followed by 24h HA addition (lane 3) or treated with Nanog siRNA plus HA for 24h (lane 4) or treated with Stat-3 siRNA plus HA for 24h (lane 5) or treated with miRNA-negative control [without HA (lane 6) or with HA for 24h (lane 7)] or treated with anti-miR-21 inhibitor plus HA for 24h (lane 8). These samples were then immunoblotted with anti-PDCD4 antibody (a) or anti-cIAP-1 antibody (b) or anti-cIAP-2 antibody (c) or anti-XIAP antibody (d), respectively. The amount of actin detected by anti-actin-mediated immunoblot (e) in each gel lane was used as a loading control.

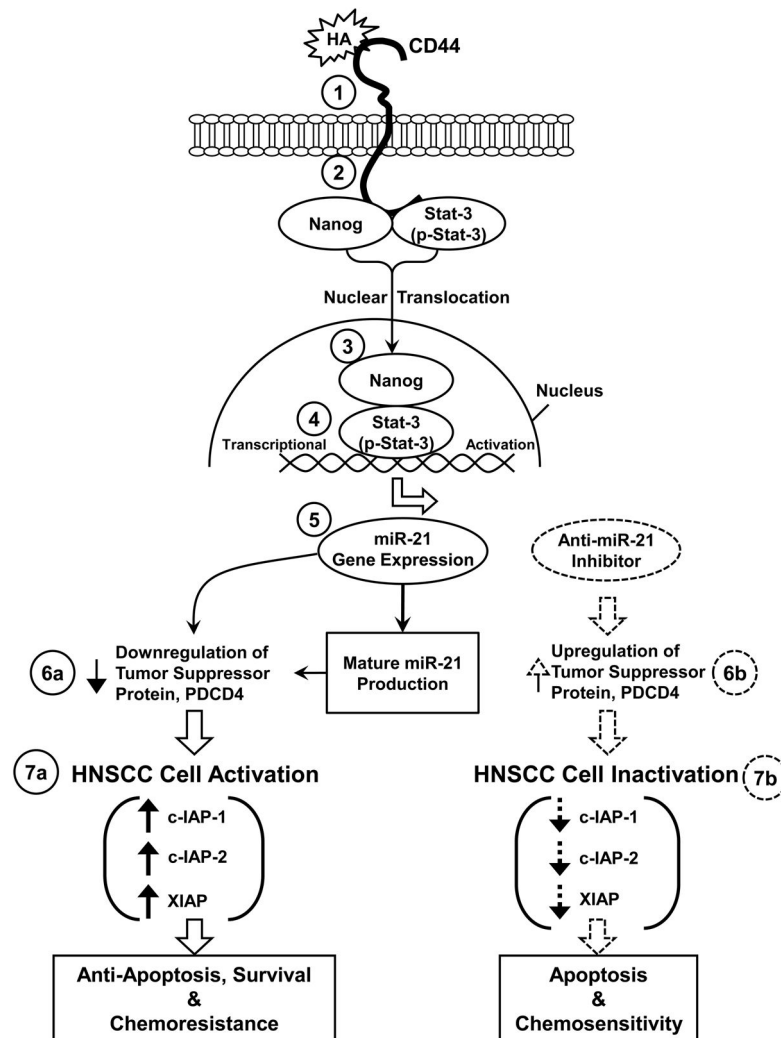


Fig. 6. A proposed model for HA/CD44-mediated Nanog and Stat-3 signaling in the regulation of miR-21 production, oncogenesis and chemoresistance in HNSCC cells

The binding of HA to CD44 (step 1) promotes a complex formation between Nanog/Stat-3 (also tyrosine phosphorylated Stat-3, p-Stat-3) and CD44 (step 2). Both Nanog and Stat-3 (p-Stat-3) then translocate from the cytosol to the nucleus and interacts with the Stat-3-binding sites located at the upstream promoter/enhancer region of miR-21 (step 4), resulting in miR-21 gene expression and mature miR-21 production (step 5). The resultant miR-21 then functions to downregulate the tumor suppressor protein (PDCD4) (step 6a, indicated by the arrow with solid lines) and promote HNSCC activation leading to IAP (c-IAP-1, c-IAP-2 and XIAP) expression, HNSCC cell anti-apoptosis/survival and chemoresistance (step 7a, indicated by the arrow with solid lines).

In direct contrast, treatment of HNSCC cells with an anti-miR-21 inhibitor induces tumor suppressor protein (PDCD4) upregulation (step 6b, indicated by the arrow with dash lines). Subsequently, these changes result in HNSCC cell inactivation including inhibition of IAP (c-IAP-1, c-IAP-2 and XIAP) expression (Fig. 7b, indicated by the arrow with dash lines), stimulation of apoptosis and enhancement of chemosensitivity in HNSCC cells. This newly-

discovered Nanog/Stat-3 signaling pathway leading to miR-21 functioning should provide important drug targets for sensitizing tumor cell apoptosis and overcome chemoresistance in HA/CD44-activated head and neck cancer cells.

Author Manuscript

Author Manuscript

Author Manuscript

Author Manuscript

Table 1A

Effects of various signaling perturbation agents on cisplatin-induced apoptosis and cell growth inhibition in HSC-3 cells.

<i>Treatments</i>	Apoptotic Cells (Annexin V-positive cell/total cells x 100%)*		Cisplatin-Induced Tumor Cell Growth Inhibition IC ₅₀ (μM)**
	No Cisplatin	+ Cisplatin	
Scrambled siRNA-treated cells (No HA)	13 ± 3	47 ± 7	1.00
Scrambled siRNA-treated cells (+ HA)	4 ± 1	9 ± 3	40.00
Scrambled siRNA + Anti-CD44-treated cells (+HA)	11 ± 2	51 ± 4	1.00
Nanog siRNA-treated cells (+ HA)	16 ± 1	86 ± 6	0.30
Stat-3 siRNA-treated cells (+ HA)	14 ± 2	71 ± 4	0.10
miRNA negative control-treated cells (No HA)	15 ± 3	55 ± 5	0.75
miRNA negative control-treated cells (+ HA)	8 ± 6	14 ± 2	30.00
Anti-miR-21 inhibitor-treated cells (+ HA)	14 ± 2	64 ± 7	0.10

* Cells were designated apoptotic when displaying Annexin V-positive staining. In each sample, at least 500 cells from five different fields were counted, with the percentage of cisplatin (2h treatment)-induced apoptotic cells calculated as Annexin V-positive cells/total number of cells. The values are presented as the means±standard deviation. All assays consisted of at least six replicates and were performed on at least 3–5 different experiments.

** Tumor cell growth inhibition (IC₅₀) is designated as “the μM concentration of chemotherapeutic drug (e.g., cisplatin-24h treatment) that causes 50% inhibition of tumor cell growth” using MTT-based growth assay as described in the Materials and Methods. IC₅₀ values are presented as the means±standard deviation. All assays consisted of at least six replicates and were performed on at least 3–5 different experiments.

Table 1B

Effects of an IAP inhibitor (SM-164) on cisplatin-induced apoptosis and cell growth inhibition in HSC-3 cells

<i>Treatments</i>	Apoptotic Cells (Annexin V-positive cell/total cells x 100%)*		Cisplatin-Induced Tumor Cell Growth Inhibition IC ₅₀ (μM)**
	No Cisplatin	+ Cisplatin	
Vehicle control-treated cells (No HA)	13 ± 2	42 ± 4	1.0
Vehicle control-treated cells (+ HA)	6 ± 3	14 ± 4	35.00
SM-164-treated cells (no HA)	27 ± 6	87 ± 6	0.05
SM-164-treated cells (+ HA)	12 ± 4	68 ± 9	0.10

* Cells were designated apoptotic when displaying Annexin V-positive staining. In each sample, at least 500 cells from five different fields were counted, with the percentage of cisplatin (2h treatment)-induced apoptotic cells calculated as Annexin V-positive cells/total number of cells. The values are presented as the means±standard deviation. All assays consisted of at least six replicates and were performed on at least 3–5 different experiments.

** Tumor cell growth inhibition (IC₅₀) is designated as “the μM concentration of chemotherapeutic drug (e.g., cisplatin-24h treatment) that causes 50% inhibition of tumor cell growth” using MTT-based growth assay as described in the Materials and Methods. IC₅₀ values are presented as the means±standard deviation. All assays consisted of at least six replicates and were performed on at least 3–5 different experiments.